

## Entanglement resonance in driven spin chains

Fernando Galve, David Zueco, Sigmund Kohler, Eric Lutz, and Peter Hänggi

*Institut für Physik, Universität Augsburg, Universitätsstraße 1, D-86135 Augsburg, Germany*

(Received 22 September 2008; revised manuscript received 5 December 2008; published 24 March 2009)

We consider a spin-1/2 anisotropic  $XY$  model with time-dependent spin-spin coupling as means of creating long-distance entanglement. We predict the emergence of significant entanglement between the first spin and the last spin whenever the ac part of the coupling has a frequency matching the Zeeman splitting. In particular, we find that the concurrence assumes its maximum with a vanishing dc part. Mapping the time-dependent Hamiltonian within a rotating-wave approximation to an effective static model provides qualitative and quantitative understanding of this entanglement resonance. Numerical results for the duration of the entanglement creation and its length dependence substantiate the effective static picture.

DOI: 10.1103/PhysRevA.79.032332

PACS number(s): 03.67.Bg, 75.10.Pq, 42.50.Hz, 62.25.Fg

### I. INTRODUCTION

Entanglement is a key resource for many quantum information and computation protocols, such as teleportation [1], superdense coding [2], and cryptography [3]. The successful storage and transfer of quantum information requires effective mechanisms to create entangled states over large distances. Since entanglement is generated mostly by local interactions, it is initially short-ranged and, thus, has to be distributed via quantum channels. Lately it has been noticed that spin chains are promising candidates for this task [4]. Various spin-spin interactions, such as, e.g., Ising or Heisenberg coupling, have been considered for entanglement creation, and their static as well as their dynamical properties have been investigated [5–9]. Spin chains thus turned out to be efficient quantum channels for controlled entanglement distribution.

A particular spin chain is the quantum anisotropic  $XY$  model. Irrespective of the magnitude of the anisotropy, it can be solved exactly with the help of a Jordan-Wigner transformation and therefore became a paradigmatic model in many-body physics [10]. In the context of quantum information [11], its experimental implementation with optical lattices [12], quantum dots [13], and Josephson junctions [14] has been proposed.

Thus far, most studies consider transfer of entanglement rather than its generation [15] or its presence in systems with static interactions [16–18]. In this paper, by contrast, we analyze a spin-1/2  $XY$  chain with periodically *time-dependent* nearest-neighbor coupling with separable initial state and find entanglement *creation* between the end spins of the chain. As it may be difficult to access individual spins in a controlled manner, we restrict ourselves to chains with global time-dependent spin-spin coupling. Remarkably, entanglement created in that way turns out to be significantly larger than the one in related static systems [19,20]. We gain further insight by mapping the time-dependent spin chain to a static model, which also provides information on the length dependence and the duration of the entanglement creation.

### II. SPIN CHAIN HAMILTONIAN

The anisotropic  $XY$  model in a transverse field  $B$  and with time-dependent nearest-neighbor coupling  $J(t)$  is described by the Hamiltonian form (we set  $\hbar=1$ ),

$$H = \frac{B}{2} \sum_{n=1}^N \sigma_n^z + \frac{J(t)}{4} \sum_{n=1}^{N-1} [(1+\gamma)\sigma_n^x \sigma_{n+1}^x + (1-\gamma)\sigma_n^y \sigma_{n+1}^y], \quad (1)$$

where the  $\sigma$ 's are the usual Pauli matrices and  $\gamma$  denotes the anisotropy parameter. We focus on situations in which the coupling strength  $J(t)$  is smaller than the field strength  $B$  and are interested in the spectral response of the chain when the coupling is periodically modulated. All other parameters have arbitrary but fixed values. We also suppose that the spins are initially uncoupled,  $J(t)=0$  for  $t<0$ , and cooled down to the fully aligned separable state,

$$|i(t=0)\rangle = |0000\cdots\rangle, \quad (2)$$

which is the ground state of Hamiltonian (1) with  $J=0$ . At  $t=0$ , we switch on a coupling consisting of a dc contribution  $J_0$  and a sinusoidal ac part with amplitude  $J_1$ ,

$$J(t > 0) = J_0 + J_1 \sin(\omega_d t). \quad (3)$$

In the limit  $J_1 \rightarrow 0$ , the coupling suddenly switches to a constant value, while for  $J_1 \neq 0$ , we are able to probe the frequency-dependent response of the system. We quantify entanglement between the two ends of the chain with the help of the concurrence  $C = \max\{\lambda_1 - \lambda_2 - \lambda_3 - \lambda_4, 0\}$ . The  $\lambda$ 's are the ordered square roots of the eigenvalues of  $\rho(\sigma_y^1 \otimes \sigma_y^2) \rho^*(\sigma_y^1 \otimes \sigma_y^2)$  with  $\rho$  being the reduced density matrix of the two spins [21].

### III. ENTANGLEMENT RESONANCE

By direct numerical integration, we investigated the time evolution of the concurrence between spins 1 and  $N$  for different driving frequencies  $\omega_d$ , chain lengths  $N$ , and parameters  $\gamma$ ,  $J_1$ , and  $J_0$ . We determined the maximal concurrence in the time interval  $[0, \dots, 4N/\max(J_0, J_1)]$ . The results shown in Fig. 1 reveal that at  $\omega_d = 2B$ , irrespective of the other parameters, the concurrence assumes during that time interval a value close to unity and is significantly larger than for other frequencies—we term this *entanglement resonance*. Height and width of the resonance peak depend on the intensities  $J_0$  and  $J_1$  and on the chain length  $N$  (see Fig. 2). We also notice the existence of a much smaller secondary peak at

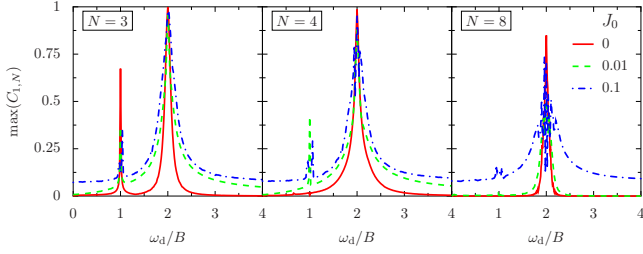


FIG. 1. (Color online) Maximum concurrence obtained in a time window up to  $4N/\max(J_0, J_1)$ , between spins 1 and  $N$  for different frequencies and chain lengths  $N$  with  $J_1=0.1B$ ,  $\gamma=1$ , and  $J_0=0$  (solid),  $0.01B$  (dashed),  $0.1B$  (dashed-dotted). The effective anisotropy thus has the values  $\tilde{\gamma}=\gamma J_1/2J_0=\infty, 5, 0.5$ .

$\omega_d=B$ . Contrary to the main peak, its amplitude strongly decreases with decreasing coupling intensity and increasing chain length. We henceforth focus on the peak at  $\omega_d=2B$ .

### Rotating-wave approximation

Deeper understanding of the observed entanglement resonance can be gained by analyzing the time-dependent Hamiltonian (1) within rotating-wave approximation. Since entanglement properties of a system are not changed by local unitary operations on individual subsystems, it is convenient to transform the XY Hamiltonian to the interaction picture,  $\tilde{H}=\exp(iH_0t)H\exp(-iH_0t)$ , with  $H_0=(B/2)\sum_i\sigma_i^z$ . By introducing the shift operators  $\sigma^\pm=\frac{1}{2}(\sigma^x\pm i\sigma^y)$ , we obtain

$$\begin{aligned} \tilde{H}(t) = & \frac{J(t)}{2} \sum_{n=1}^N [\sigma_n^+ \sigma_{n+1}^- + \sigma_{n+1}^+ \sigma_n^- + \gamma e^{2iBt} \sigma_n^+ \sigma_{n+1}^+ \\ & + \gamma e^{-2iBt} \sigma_n^- \sigma_{n+1}^-]. \end{aligned} \quad (4)$$

The first two terms swap excitations of spins  $n$  and  $n+1$ , while the last two terms pairwise create (destroy) excitations, which here are the origin of entanglement generation. If the driving frequency obeys the resonance condition  $\omega_d=2B$  and, moreover, is much larger than both  $J_0$  and  $J_1$ , we can within rotating-wave approximation (RWA) replace Hamiltonian (4) by its time average,

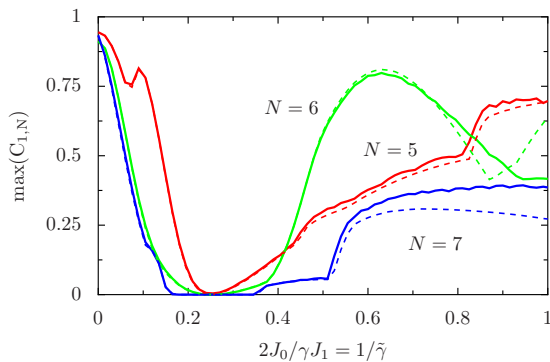


FIG. 2. (Color online) Maximum obtained concurrence between the end spins for  $\omega_d=2B$  as a function of the dc interaction  $J_0$  for various chain lengths,  $J_1=0.1B$  and  $\gamma=1$ . The solid lines are obtained with the full time-dependent Hamiltonian (1), while the dashed lines mark the RWA solution.

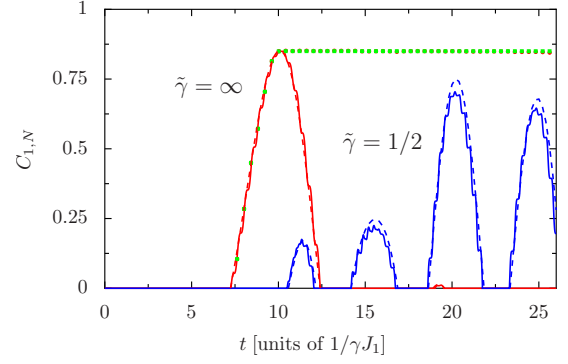


FIG. 3. (Color online) Entanglement dynamics for a chain of eight spins with driving frequency  $\omega_d=2B$  for two different effective anisotropies  $\tilde{\gamma}=\gamma J_1/2J_0$ . As in Fig. 1,  $J_1=0.1B$ ,  $\gamma=1$ . Solid lines mark the exact numerical solution, while the dashed lines are computed within RWA. The symbols mark the time evolution for switching off the driving (squares) and for changing the frequency to  $\omega=3B$  (circles) after the concurrence maximum is reached at time  $t_{\text{arrival}}$ . Both results cannot be distinguished for the chosen resolution.

$$\tilde{H}_R = \frac{J_0}{2} \sum_{n=1}^N [\sigma_n^+ \sigma_{n+1}^- + \tilde{\gamma} \sigma_n^+ \sigma_{n+1}^+ + \text{H.c.}] \quad (5)$$

with the effective anisotropy  $\tilde{\gamma}=\gamma J_1/2J_0$ . This means that for resonant driving, the time-dependent XY model (1) can be mapped to the static XY model (5) without any Zeeman field. In both cases, the entanglement generated between the two end spins is maximal and controlled by the parameter  $\tilde{\gamma}$  and the chain length  $N$ . Note that  $J_0 \rightarrow 0$  corresponds to the infinitely anisotropic limit  $\tilde{\gamma} \rightarrow \infty$ . Figure 2 shows the concurrence between the end spins as a function of the anisotropy parameter  $\tilde{\gamma}$  for resonant driving. Two important points are worth being mentioned. First, the concurrence approaches unity in the limit of vanishing  $J_0$ , i.e., for infinite  $\tilde{\gamma}$ . In this limit, the amount of entanglement no longer depends on  $J_1$  and  $\gamma$ . Second, the agreement of the exactly evaluated concurrence and the RWA solution is excellent, which demonstrates that RWA is appropriate. Moreover, Fig. 3 shows that this approximation also captures the entanglement dynamics, besides some small oscillations stemming from neglected rapidly oscillating terms.

## IV. ENTANGLEMENT DYNAMICS FOR RESONANT DRIVING

In order to investigate the entanglement dynamics, we consider the exact time evolution and discuss it within RWA. In doing so, we find that the value of the effective anisotropy parameter  $\tilde{\gamma}$  determines the qualitative behavior.

### A. Strong anisotropy

For a three-spin chain in the limit  $\tilde{\gamma} \rightarrow \infty$  ( $J_0=0$ ), the repeated action of Hamiltonian (5) on the initial state creates the cyclic sequence  $|000\rangle \rightarrow |110\rangle + |011\rangle \rightarrow |000\rangle$ . This implies that the quantum dynamics is a coherent oscillation between only these two states. The corresponding concu-

rence reads  $C_{1,3} = |\sin(\gamma J_1/2\sqrt{2}t)|$ . In particular, at certain times, spins 1 and 3 are fully entangled,  $C_{1,3} = 1$ . The exact time evolution (not shown) agrees very well with the RWA prediction. The three-spin case also reveals the difference between an open and a closed chain: for the closed chain, which is translation invariant, the fully entangled state  $|110\rangle + |011\rangle$  would be replaced by  $|110\rangle + |011\rangle + |101\rangle$  which has lower bipartite concurrence. This emphasizes that lack of translation invariance supports the entanglement creation between the ends of the chain.

For longer chains, the situation becomes more involved but still can be understood qualitatively. Because the Hamiltonian conserves parity and the initial state has zero excitations, the system will remain at all times in a subspace of states having an even number of excitations. This together with the fact that the chain is open can be used to argue why at resonance there is such a huge amount of entanglement. Further, this argument also leads to the conclusion that at the point of maximum entanglement, the reduced state of spins in the ends of the chain is  $(|00\rangle + |11\rangle)/\sqrt{2}$  for even chains and  $(|01\rangle + |10\rangle)/\sqrt{2}$  for odd chains, plus a mixed state contribution which is smallest the highest the concurrence. A more detailed argumentation can be read in the Appendix.

The resulting entanglement dynamics is shown in Fig. 3: we find that the concurrence begins to grow after a given time and reaches a maximum value at a time  $t_{\text{arrival}}$ . Thereafter, it decays. However, two ways of maintaining the achieved concurrence come to mind: one can either simply switch off the driving, i.e.,  $J(t > t_{\text{arrival}}) = 0$ , or shift the driving frequency to an off-resonant value  $\omega_d \neq 2B$ . The dotted lines in Fig. 3 show that both strategies freeze the entanglement as desired. This certainly requires knowledge of  $t_{\text{arrival}}$  which behaves very regularly and can be well estimated, as we demonstrate below. Moreover, switching off the driving parameters has to be much faster than the typical time scale of the system, as we assume throughout this work. The same applies also to the onset of the driving.

### B. Moderate anisotropy

For finite anisotropy  $\tilde{\gamma} (J_0 \neq 0)$ , the dynamics becomes rather complex (see Fig. 3). The concurrence assumes several local maxima until the highest one is reached. Moreover, we find that the concurrence maximum became lower. This is due to the presence of swapping terms, which spoil the argumentation of the Appendix. These terms basically will mix the subsets  $\{|00\rangle, |11\rangle\}$  and  $\{|01\rangle, |10\rangle\}$  and thus reduce the maximum achievable amount of concurrence.

Thus, we can conclude that the anisotropic limit  $\tilde{\gamma} \rightarrow \infty$  ( $J_0 = 0$ ) is the optimal working point and, henceforth, restrict our discussion to this limit.

## V. SCALABILITY AND ARRIVAL TIME

Our next goal is to find the arrival time  $t_{\text{arrival}}$  and the corresponding concurrence maximum as a function of the chain length  $N$ . Direct integration of the time-dependent Schrödinger equation was only possible for up to 12 spins. The solution for eight spins, however, already demonstrates

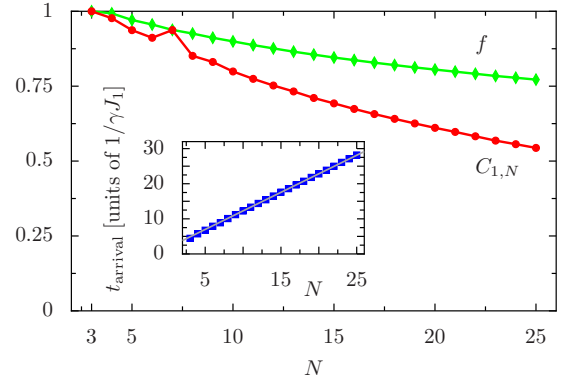


FIG. 4. (Color online) Length dependence of the first maximum of the concurrence between ends,  $C_{1,N}(t)$ , and the corresponding fully entangled fraction  $f$  for RWA Hamiltonian (5) with  $J_0 = 0$ . The inset shows the length dependence of the arrival time at which the entanglement assumes its maximum.

that for  $\omega_d = 2B$ , the RWA Hamiltonian (5) captures the global behavior very well (see Fig. 3). Therefore, we can make even further progress by mapping the RWA Hamiltonian to a model for which an exact solution is known. For the unitary transformation  $\mathcal{S} = \prod_{i=1,3,\dots} \sigma_i^x$  which flips the spins with odd site number, we find the duality relation

$$\tilde{\gamma} \tilde{H}_{\tilde{\gamma}=0} = \tilde{S} \tilde{H}_{J_0=0} \tilde{S}^\dagger. \quad (6)$$

This means that the Hamiltonian for the infinitely anisotropic case can be cast as a scaled isotropic Hamiltonian, while our initial state is mapped to the Néel state:  $|1010\cdots\rangle = \mathcal{S}|0000\cdots\rangle$ . The Hamiltonian  $\tilde{H}_{\tilde{\gamma}=0}$  can be diagonalized after a Jordan-Wigner transformation [22].

Figure 4 shows that the maximum entanglement achieved decreases with the chain length rather slowly. For very short chains we find almost perfect entanglement, as predicted above within RWA, while for length  $N = 25$ , the concurrence still possesses the appreciable value  $C_{1,25} \approx 0.5$ . A typical figure of merit in communication protocols is the “fully entangled fraction,” defined as  $f = \max\langle e | \rho | e \rangle$ , where  $\{|e\rangle\}$  is the set of all maximally entangled states [23]. Quantum communication protocols are superior to their classical counterparts whenever this fraction is higher than  $2/3$ . In Fig. 3 it is seen that this magnitude greatly surpasses the classical efficiency for rather long chains.

Note that a chain of length  $N = 7$  represents a particular case in which the concurrence equals the fully entangled fraction. We cannot provide an intuitive explanation for this anomalous behavior.

Already above, we mentioned the importance of knowing the time  $t_{\text{arrival}}$  at which the concurrence assumes its maximum. In the strongly anisotropic limit  $\tilde{\gamma} \rightarrow \infty$  ( $J_0 = 0$ ), we can provide a good estimate for the arrival time with the following reason: a typical local excitation will be transported with group velocity  $v_k = d\epsilon_k/dk$ , where for  $J_0 = 0$ , the eigenenergies  $\epsilon_k = (\gamma J_1/2)\cos(k)$  are determined by the wave number  $k = \pi m/(N+1)$ ,  $m = 1, \dots, N$ , and form a band. Since the initial state  $|0000\cdots\rangle$  is located in the center of the band, the

relevant wave number is  $k \approx \pi/2$ . Thus, the time scale for traversing the chain is

$$t^* = \frac{N}{v_{\pi/2}} = \frac{2N}{\gamma J_1}. \quad (7)$$

The inset of Fig. 3 shows that

$$t_{\text{arrival}} \approx \frac{1.7}{\gamma J_1} + \frac{t^*}{2} = \frac{1.7 + N}{\gamma J_1}, \quad (8)$$

i.e.,  $t_{\text{arrival}}$  grows linearly with the chain length. The factor  $1/2$  on  $t^*$  reflects the fact that counterpropagating excitations will meet already in the middle of the chain thus establishing distant entanglement.

Recently, Wichterich and Bose [24] computed the fully entangled fraction in spin chains with isotropic nearest-neighbor interaction. Starting from the mixed Néel state  $(1/2)|0101\cdots\rangle\langle 0101\cdots| + (1/2)|1010\cdots\rangle\langle 1010\cdots|$ , they found that switching on a constant interaction entangles the spins located at the end sites. The unitary transformation (6) maps this model to the limit  $\tilde{\gamma} \rightarrow \infty$  of the RWA Hamiltonian (5). Moreover, our discussion of the entanglement dynamics within RWA vividly explains why in their case the isotropic model permits the creation of a remarkably high entanglement.

## VI. IMPLEMENTATION WITH OPTICAL LATTICES

The realization of an XY chain with anisotropy  $\gamma=1$  has been proposed for experiments with cold atoms in a one-dimensional optical lattice that in transverse direction forms a bistable potential [12]. The ground-state doublet of each double-well forms the “spin” degree of freedom. Then our initial state (2) corresponds to a Mott-insulator state, which has already been realized experimentally [25]. There the tunnel barriers in longitudinal direction can be up to  $\sim 22E_r$ , where the recoil energy  $E_r$  typically lies in the kilohertz regime. This is more than sufficient for suppressing longitudinal tunneling, such that each double well remains occupied with a single atom. The spin-spin interaction is given by a Bose-Hubbard repulsion term caused by an overlap of Wannier functions describing neighboring atoms. The amount of overlap is given by the barrier height, which can be controlled and modulated via the laser intensity, yielding a time dependent  $J(t)$ . Thus a high barrier effectively yields no overlap and hence no spin-spin interaction ( $J=0$ ), whereas a low barrier can yield values  $J \sim 0.1$  kHz [26]. The Zeeman field  $B$  corresponds to the tunnel splitting of the double-well potential and is of the order  $0.1E_r$  [27], though it can be manipulated by changing the depth of the double-well potential so that  $B$  is greater than, but of the order of  $J(t)$ . This implies that the switching times of the Zeeman fields have to be considerably smaller than 1 ms. Coherence times for atoms in such optical lattices can be much larger than the system time scale and, thus, decoherence should not play a major role. Moreover, the initial state  $|000\cdots 0\rangle$  can be imposed by tailoring the field  $B$  to be much higher than thermal excitation energy  $k_B T$  due to the environment. Finally, the “spin state” in the transverse double well can be probed by fluorescence measurement of the atoms.

## VII. CONCLUSIONS

We have shown that proper ac driving can induce almost perfect entanglement between the end spins of an anisotropic XY chain. As a most striking feature, we found that the driven chain bears the potential for a considerably larger entanglement than the formerly studied static chains. We identified a resonance condition which leads to maximal entanglement and also provide a reliable estimate for the time after which this entanglement is reached. The latter is crucial for freezing the entanglement once it is created. Our analysis within a rotating-wave approximation contributed to a qualitative and quantitative understanding of how the entanglement is built up: pairwise flipping of neighboring spins of an open chain favors correlations between the end spins. Moreover, we found that the maximum entanglement decreases only weakly with the chain length, while the entanglement is built up during a time that is linearly length dependent. Thus our protocol demonstrates good scalability which is a major requirement for the implementation of quantum communication protocols. A natural application of our scheme is quantum communication via state teleportation. This is possible because the fully entangled fraction between the first spin and the last spin is sufficiently large, such that a spin singlet can be purified [23]. Let us finally emphasize that our protocol can be implemented with three different experimental setups, namely, an anisotropic chain with sinusoidal driving, an infinitely anisotropic chain with a sudden switch, and an isotropic chain with initial Néel state. This provides a broad choice for its application.

## ACKNOWLEDGMENTS

We gratefully acknowledge support by the German Excellence Initiative via the “Nanosystems Initiative Munich (NIM),” as well as by DFG through SFB 484 and SFB 631, and the Emmy Noether program under Grant No. LU1382/1-1.

## APPENDIX: ENTANGLEMENT IN STRONGLY ANISOTROPIC CHAINS

Due to the parity preserving character of the Hamiltonian and the fact that our initial state  $|00\cdots 0\rangle$  has a definite parity, the reduced density matrix of the spins at the ends of the chain  $\rho_R$  is of the form  $p_1|00\rangle\langle 00| + p_2(|01\rangle\langle 01| + |10\rangle\langle 10|) + p_3|11\rangle\langle 11| + (\alpha|00\rangle\langle 11| + \beta|01\rangle\langle 10| + \text{H.c.})$ . In the basis  $\{|00\rangle, |01\rangle, |10\rangle, |11\rangle\}$ , it reads

$$\rho_R = \begin{pmatrix} p_1 & 0 & 0 & \alpha \\ 0 & p_2 & \beta & 0 \\ 0 & \beta^* & p_2 & 0 \\ \alpha^* & 0 & 0 & p_3 \end{pmatrix}, \quad (A1)$$

and the corresponding concurrence is

$$C = 2 \max(0, |\alpha| - p_2, |\beta| - \sqrt{p_1 p_3}). \quad (A2)$$

Because the chain is open and the Hamiltonian flips spins pairwise at adjacent sites, we find  $\beta=0$  for even chains and  $\alpha=0$  for odd chains.

For even chains, the proof of this statement is as follows: the term  $|01\rangle\langle 10|$  stems from evaluating the trace over density operators of the form  $|0[x]1\rangle\langle 1[y]0|$ , where the blocks  $[x]$  and  $[y]$  represent the rest of the chain. Obviously, only terms with  $[x]=[y]$  yield a nonvanishing contribution. We demonstrate by *reductio ad absurdum* that it is impossible to fulfill this condition: let us assume that states  $|0[x]1\rangle\langle 1[x]0|$  can occur. By applying to this state Hamiltonian (5) which for strong anisotropy flip spins pairwise, we obtain  $[x]=[y]1$  for the ket and  $[x]=1[z]$  for the bra, where the blocks  $[y]$  and  $[z]$  are yet one spin shorter and, thus, consist of an odd number of spins. Hence  $[x]=1[x']1$ , such that the operator becomes  $|01[x']1\rangle\langle 11[x']10|$ . Again, by the same reasoning we find the requirement  $[x']=1[y']$  for the ket and  $[x']=[z']1$  for the bra. Therefore  $[x']=1[x'']1$  and, thus,  $|011[x'']1\rangle\langle 111[x'']10|$ . Repeating this procedure, we end up with a collection of ever smaller blocks  $[x], [x'], [x''], \dots, [x^{(n)}]$  all of which possess an even number of spins. Eventually, we remain with the operator  $|011\cdots 1[x^{(n)}]1\rangle\langle 11\cdots 1[x^{(n)}]1\rangle$ . From the ket we

find the condition that  $[x^{(n)}]=[10]$ , while from the bra follows  $[x^{(n)}]=[01]$  in order to have an even number of spins in state 1, i.e., to conserve parity. Thus we can conclude that the initial hypothesis  $[x]=[y]$  must be wrong. This proves that for even chains  $\beta=0$ , and so the concurrence reduces to  $C=2 \max(0, |\alpha|-p_2)$ . This line of reasoning can be adapted to the case of odd chains, for which one obtains  $\alpha=0$ .

Yet, in order to obtain a high concurrence, we need  $|\alpha| \gg p_2$ , as we find in our numerical studies. The trace condition for density matrices yields  $p_1+p_3=1-2p_2$ , while positivity requires  $|\alpha| \leq \sqrt{p_1 p_3}$ . Note that for pure states,  $|\alpha| = \sqrt{p_1 p_3}$ . Thus, maximizing  $\alpha$  necessarily requires  $p_2$  be small, that is, if at any instance of time,  $\alpha$  starts to increase, as it happens when  $p_2$  becomes smaller, the concurrence increases as well. Clearly this can occur only at certain times, which is why we see entanglement peaks.

At times of maximum concurrence, the resulting state shared between spins 1 and  $N$  is then  $a_1|00\rangle+a_2|11\rangle$  for even chains and  $a_1|01\rangle+a_2|10\rangle$  for odd chains, where we have ignored a small mixed state contribution.

- 
- [1] C. H. Bennett, G. Brassard, C. Crepeau, R. Jozsa, A. Peres, and W. K. Wootters, Phys. Rev. Lett. **70**, 1895 (1993).
- [2] C. H. Bennett and S. J. Wiesner, Phys. Rev. Lett. **69**, 2881 (1992).
- [3] A. K. Ekert, Phys. Rev. Lett. **67**, 661 (1991).
- [4] S. Bose, Phys. Rev. Lett. **91**, 207901 (2003).
- [5] L. Amico, A. Osterloh, F. Plastina, R. Fazio, and G. M. Palma, Phys. Rev. A **69**, 022304 (2004).
- [6] J. Fitzsimons and J. Twamley, Phys. Rev. Lett. **97**, 090502 (2006).
- [7] F. Plastina and T. J. G. Apollaro, Phys. Rev. Lett. **99**, 177210 (2007).
- [8] T. S. Cubitt and J. I. Cirac, Phys. Rev. Lett. **100**, 180406 (2008).
- [9] A. O. Lyakhov and C. Bruder, Phys. Rev. B **74**, 235303 (2006).
- [10] E. Lieb, T. Schultz, and D. Mattis, Ann. Phys. **16**, 407 (1961).
- [11] L. Amico, R. Fazio, A. Osterloh, and V. Vedral, Rev. Mod. Phys. **80**, 517 (2008).
- [12] U. Dorner, P. Fedichev, D. Jaksch, M. Lewenstein, and P. Zoller, Phys. Rev. Lett. **91**, 073601 (2003).
- [13] A. Imamoglu, D. D. Awschalom, G. Burkard, D. P. DiVincenzo, D. Loss, M. Sherwin, and A. Small, Phys. Rev. Lett. **83**, 4204 (1999).
- [14] Y. Makhlin, G. Schön, and A. Shnirman, Rev. Mod. Phys. **73**, 357 (2001).
- [15] S. Bose, Contemp. Phys. **48**, 13 (2007).
- [16] L. Campos Venuti, C. Degli Esposti Boschi, and M. Roncaglia, Phys. Rev. Lett. **96**, 247206 (2006).
- [17] A. Ferreira and J. M. B. Lopes dos Santos, Phys. Rev. A **77**, 034301 (2008).
- [18] C. Di Franco, M. Paternostro, and M. S. Kim, Phys. Rev. A **77**, 020303(R) (2008).
- [19] K. M. O'Connor and W. K. Wootters, Phys. Rev. A **63**, 052302 (2001).
- [20] A. Osterloh, L. Amico, G. Falci, and R. Fazio, Nature (London) **416**, 608 (2002).
- [21] W. K. Wootters, Phys. Rev. Lett. **80**, 2245 (1998).
- [22] H. J. Mikeska and W. Pesch, Z. Phys. B **26**, 351 (1977).
- [23] C. H. Bennett, D. P. DiVincenzo, J. A. Smolin, and W. K. Wootters, Phys. Rev. A **54**, 3824 (1996).
- [24] H. Wichterich and S. Bose, e-print arXiv:0806.4568.
- [25] M. Greiner, O. Mandel, T. Esslinger, T. W. Hänsch, and I. Bloch, Nature (London) **415**, 39 (2002).
- [26] L.-M. Duan, E. Demler, and M. D. Lukin, Phys. Rev. Lett. **91**, 090402 (2003).
- [27] O. Morsch and M. Oberthaler, Rev. Mod. Phys. **78**, 179 (2006).